Dissociation of Ca^{2+} from Sarcoplasmic Reticulum Ca^{2+}-ATPase and Changes in Fluorescence of Optically Selected Trp Residues. Effects of KCl and NaCl and Implications for Substeps in Ca^{2+} Dissociation†

Philippe Champeil,*,‡ Fernando Henao,§ and Béatrice de Foresta‡

Unité de Recherche 2096 Associée au Centre National de la Recherche Scientifique and Section de Biophysique des Protéines et des Membranes, Département de Biologie Cellulaire et Moléculaire, Commissariat à l'Energie Atomique, Centre d'Etudes de Saclay, 91191 Gif-sur-Yvette Cedex, France, and the Departamento de Bioquímica y Biología Molecular, Facultad de Ciencias, Universidad de Extremadura, 06080 Badajoz, Spain

Received April 24, 1997; Revised Manuscript Received June 25, 1997⊗

ABSTRACT: Sequential dissociation of the two Ca^{2+} ions bound to non-phosphorylated sarcoplasmic reticulum Ca^{2+}-ATPase was triggered by addition, in a stopped-flow experiment, of quin2, which acted both as a high-affinity chelator and as a Ca^{2+}-sensitive fluorescent probe. The kinetics of Ca^{2+} dissociation were deduced from the observed changes in quin2 fluorescence in the visible region (with $\lambda_{ex} = 313$ nm), while fluorescence detection in the UV region (with $\lambda_{ex} = 290$ nm) made it possible to monitor the tryptophan fluorescence changes accompanying this dissociation under the same ionic conditions. In the absence of KCl or NaCl, at pH 6 or 7, the observed changes in quin2 fluorescence were monoexponential, with rate constants very close to those of the changes in ATPase tryptophan fluorescence, which also appeared monophasic. In the presence of 100 mM KCl, quin2 fluorescence changes, although still monoexponential, were faster than in the absence of the monovalent ions but distinctly slower than the changes in tryptophan fluorescence, which were accelerated to a larger extent. In addition, the apparent kinetics of the Trp fluorescence changes depended on the excitation wavelength. Using an excitation wavelength of 296 nm, the Trp fluorescence drop was still faster than with an excitation wavelength of 290 nm, and in the presence of NaCl it even displayed a clear undershoot. We conclude that in the presence of KCl or NaCl and with an excitation wavelength of 290 nm, the rapid drop in tryptophan fluorescence mainly monitors the dissociation of the first of the two Ca^{2+} ions to be released from Ca^{2+}-ATPase, while excitation at 296 nm optically selects a subpopulation of Trp residues whose fluorescence level is *lower* in the ATPase species with one Ca^{2+} ion bound than in the Ca^{2+}-deprived ATPase species. The latter conditions result in an initial drop in Trp fluorescence whose apparent rate constant (in single-exponential analysis) is faster than the true rate of dissociation of the first Ca^{2+} ion and in a subsequent slower rise related to dissociation of the second Ca^{2+} ion. The difference between results obtained in the absence and in the presence of K^+ or Na^+ is due to an antagonizing effect of these cations on proton-induced conformational rearrangement of Ca^{2+}-free ATPase, a conformational rearrangement which changes the ATPase Trp fluorescence level and significantly affects the cooperativity of Ca^{2+} binding at equilibrium.

The Ca^{2+}-ATPase present in sarcoplasmic reticulum is a membrane protein which catalyzes the transport of two Ca^{2+} ions per hydrolyzed ATP molecule (*1*−*5*). Ca^{2+} binding to its high-affinity binding sites on non-phosphorylated ATPase induces critical conformational changes for the ATPase: the ATPase with bound Ca^{2+} can subsequently react with ATP but not with inorganic phosphate, whereas Ca^{2+}-free ATPase can react with P_i but not with ATP (*2,6*). These conformational changes have been a subject of interest for many years, and they have been often studied *via* the accompanying changes in spectroscopic probes of the ATPase structure (*7*). In particular, the changes in ATPase intrinsic fluorescence, due to thirteen Trp residues present on each polypeptide chain, have offered a convenient way to monitor the *kinetics* of these changes in stopped-flow experiments (*8*−*11*); rapid filtration experiments with $^{45}Ca^{2+}$ have subsequently made it possible to directly study the kinetics of binding or dissociation of Ca^{2+} (*12,13*). Measuring these kinetics accurately is an important issue: the kinetics observed for the events depending on Ca^{2+} *binding* have been discussed in terms of reaction models for the ATPase, to try to discriminate whether conformational rearrangement of ATPase follows or precedes Ca^{2+} binding and whether a monomeric or an oligomeric structure for the ATPase fits best with the data (*9,10,14*−*20*); simultaneously, the detailed kinetics of Ca^{2+} *dissociation*, which were found to be

† Part of this work was presented at the 41st Annual Meeting of the Biophysical Society, March 2-6, 1997, New Orleans, LA.

* Corresponding author.
‡ Centre d'Etudes de Saclay.
§ Universidad de Extremadura.

⊗ Abstract published in *Advance ACS Abstracts,* August 15, 1997.

[1] Abbreviations: SR, sarcoplasmic reticulum; ATPase, adenosine triphosphatase; quin2, 2-[(2-amino-5-methylphenoxy)methyl]-6-methoxy-8-aminoquinoline-*N*,*N*,*N*′,*N*′-tetraacetic acid; EGTA, [ethylenebis-(oxyethylenenitrilo)]tetraacetic acid; EDTA, ethylenediaminetetraacetic acid; Mes, 2-(*N*-morpholino)ethanesulfonic acid; Mops, 4-morpholinepropanesulfonic acid; Tris, tris(hydroxymethyl)aminomethane; FITC, fluorescein 5′-isothiocyanate; Trp, tryptophan; λ_{ex} and λ_{em}, excitation and emission wavelengths, respectively; bw, spectral bandwidth; E, ECa, ECa_2, ATPase species with zero, one, or two Ca^{2+} ions bound to the transport sites.

S0006-2960(97)00969-0 CCC: $14.00

Table 1: Dissociation Constants Used in This Study

metal−chelator (ionic conditions)	apparent or combined dissociation constant		
	pH 6	pH 7	pH 8
Mg−EGTA ($\mu_i = 0.1$ M)	4×10^{-1} M	3.4×10^{-2} M	
Ca−EGTA ($\mu_i = 0.1$ M)	3.8×10^{-5} M	3.8×10^{-7} M	3.8×10^{-9} M
Ca−EGTA ($\mu_i = 0.1$ M, 5 mM Mg^{2+})		4.5×10^{-7} M	
Ca−quin2 (100 mM KCl, 50 mM Mops-Tris)	4×10^{-7} M	1.4×10^{-7} M	0.8×10^{-7} M
Ca−quin2 (100 mM KCl, 50 mM Mops-Tris, 5 mM Mg^{2+})	6×10^{-7} M	3.2×10^{-7} M	
Ca−quin2, (KCl = 0, 150 mM Mops-Tris)	3×10^{-7} M		
Ca−[Mg−EDTA] ($\mu_i = 0.1$ M, 5 mM Mg^{2+})		6.2×10^{-5} M	

[a] The apparent or combined (*41*,*42*) dissociation constants for EGTA were *computed* from the constants given in (*43*) for 0.1 M ionic strength (μ_i). The apparent affinity of Ca^{2+} for "Mg−EDTA", i.e. for EDTA in the presence of 5 mM excess free Mg^{2+}, was also computed (*44*−*46*). On the basis of the computed constants for Ca−EGTA, we then *measured* the affinity of quin2 for Ca^{2+} under various conditions [see also (*29*)].

sequential, have been discussed in structural terms for the binding pocket, implying the co-existence in a channel-like single-file crevice of a more superficial binding site and a more deeply embedded one [both indirect chemical quenching and direct $^{45}Ca^{2+}$ filtration results (*12*,*13*,*21*−*25*) have been reported].

A few studies have compared the kinetics of Ca^{2+}-dependent changes in ATPase Trp fluorescence, as measured by stopped-flow fluorescence experiments, with the kinetics of $^{45}Ca^{2+}$ dissociation itself, as measured by rapid filtration experiments; these studies concluded that the drop in Trp fluorescence accompanying Ca^{2+} dissociation is a reasonable index of this dissociation (*12*,*18*,*19*,*25*). This conclusion was extended to conditions where the Trp changes are faster and can no longer easily be compared to rapid filtration experiments (which have a dead time of 20−30 ms, compared with 3−4 ms for stopped-flow experiments); for instance, the large accelerating effect of K^+ on Trp fluorescence changes observed at neutral pH, as well as the effect of pH itself on these changes, was attributed to a true effect on Ca^{2+} dissociation (*25*−*27*). At pH 6, however, we had directly measured the effect of K^+ on $^{45}Ca^{2+}$ dissociation in $^{45}Ca^{2+}$ filtration studies and had observed only slight acceleration (*25*). It therefore appeared necessary to reassess the correlation between Trp fluorescence changes and Ca^{2+} dissociation under a variety of conditions.

To do this, we resorted to a previously established technique (*28*) to measure Ca^{2+} dissociation in the presence of the high-affinity fluorescent chelator quin2 [compound **3b** in (*29*)]. Using different combinations of excitation and emission conditions in stopped-flow fluorescence experiments, we could alternatively monitor the changes in quin2 fluorescence (i.e., Ca^{2+} dissociation) and the accompanying changes in Trp fluorescence under exactly the same ionic conditions. The results described in this work show that, under certain ionic conditions, the Trp fluorescence changes exactly parallel overall Ca^{2+} dissociation from the ATPase, but this is not the case under all ionic conditions, especially in the presence of KCl, a common situation. We also found that, among the thirteen Trp residues in ATPase, some can be optically selected by using an excitation wavelength on the red edge of the Trp excitation spectrum and that these residues respond in a specific way to dissociation of the first and the second of the two Ca^{2+} ions released from the ATPase. Measurements performed under equilibrium conditions are fully consistent with these time-resolved results. Implications for the substeps in Ca^{2+} dissociation and the resulting changes in Trp fluorescence, as well as for future localization of the various Trp residues in ATPase, are described. Part of this work was presented at the 41st Annual Meeting of the Biophysical Society in New Orleans, LA (*30*).

EXPERIMENTAL PROCEDURES

The procedures used for SR vesicle preparation as well as for $^{45}Ca^{2+}$ binding measurements have already been described (*25*). The free Ca^{2+} concentration in the various solutions was estimated with the dissociation constants given in Table 1. Ca^{2+}-ATPase was labeled with FITC as previously described (*31*). The fluorescent chelator quin2 (potassium salt) was obtained from Calbiochem. All other chemicals were analytical grade.

Fluorescence Measurements

Fluorescence measurements at equilibrium were performed with a Spex fluorolog fluorometer, an SLM 4000, or an SLM 8000. Most time-resolved fluorescence measurements were performed with a Biologic SFM 3 stopped-flow instrument equipped with a short-pathlength optical cell (1.5 mm, "FC15" cell), illuminated through a high-resolution grating and an optical fiber, the physical width of which limited the spectral bandwidth of the excitation beam to less than 1 nm. Other experiments were performed with a Dionex D110 system illuminated through a monochromator with a wide spectral bandwidth [4 nm as in (*10*)]. Stopped-flow fluorescence data were fitted to single or multi-exponentials using a Simplex routine (Biologic); in all cases the presence of a small (linear) drift, mainly due to photolysis, was taken into account. To detect emitted fluorescence, we used wide band filters centered in the region of either quin2 or Trp fluorescence, obtained from Ealing Optics (S. Natick, MA) and from MTO (Massy, France) (see figure legends).

Use of quin2 to Measure the Rate of Ca^{2+} Dissociation from Ca^{2+}-ATPase

We adapted a previously described protocol (*28*), which has often been used to measure the kinetics of Ca^{2+} dissociation from soluble Ca^{2+}-binding proteins (*32*−*36*) but only once to measure Ca^{2+} dissociation from a membrane protein (*17*). The rationale of these measurements is as follows. When quin2, present at a high concentration in one of the syringes of a stopped-flow system, is mixed with the contents of the other syringe, it rapidly binds Ca^{2+} ions available in solution within the dead time of the stopped-flow system (a few milliseconds), and the kinetics of the corresponding rise in quin2 fluorescence are not resolved.

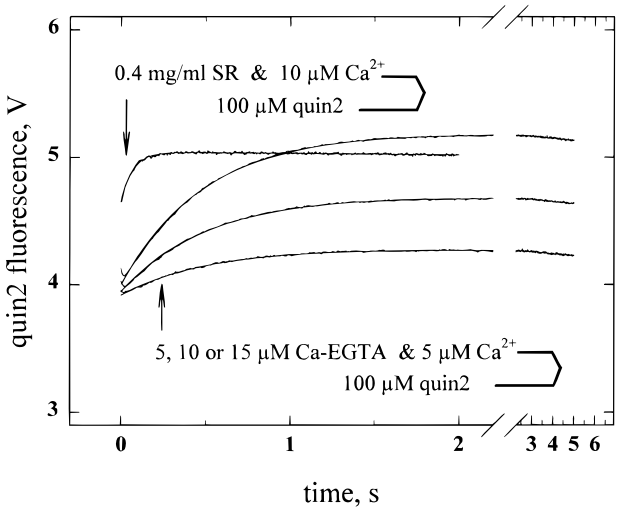

FIGURE 1: Changes in quin2 fluorescence observed after mixing quin2 with either Ca^{2+}-equilibrated SR vesicles or various amounts of Ca−EGTA complexes. For the experiment illustrated by the top trace, 10 μM Ca^{2+} and 0.4 mg of protein/mL of SR vesicles (in this particular experiment, Ca^{2+}-ATPase in the SR vesicles had been previously labeled with FITC, but similar results were obtained with unlabeled vesicles) were mixed in a one to one volume ratio with 100 μM quin2; the medium contained 100 mM KCl and 50 mM Mops-Tris at pH 7 and 20 °C. For the three bottom traces, 5 μM Ca^{2+} and 5, 10 or 15 μM of Ca−EGTA were mixed with quin2. To monitor quin2 fluorescence the excitation wavelength was set at 313 nm; in this particular experiment, a wide-band filter centered at 450 nm (Ealing 35−5024) was used to detect emitted quin2 fluorescence while rejecting FITC fluorescence. The collected data are shown together with their fit to single exponentials (plus a constant photolysis rate). The rate constants and amplitudes of these exponentials are as follows: for SR Ca^{2+}-ATPase, 15 s^{-1} and 0.395 V; for 5, 10, or 15 μM Ca−EGTA, 1.98 s^{-1} and 0.39 V, 1.93 s^{-1} and 0.78 V, or 1.90 s^{-1} and 1.23 V, respectively.

A very low free Ca^{2+} concentration is established. If, on a slower time scale, Ca^{2+} ions subsequently dissociate from a complex previously present in that other syringe, then the released Ca^{2+} ions will also bind to quin2, resulting in an additional rise in quin2 fluorescence, the rate of which will exactly match the rate of Ca^{2+} dissociation from the complex. The amplitude of this final rise is linearly related to the amount of Ca^{2+} released from the complex because virtually all released Ca^{2+} ions bind to quin2, present at a final concentration well above its K_d. Figure 1 shows two examples of these experiments in which quin2 was mixed either with Ca^{2+}-equilibrated SR vesicles (top trace) or with Ca−EGTA complexes at three different concentrations (bottom traces). From such experiments, the amplitude of the quin2 fluorescence trace can be calibrated in terms of Ca^{2+} concentrations. We found that 12 ± 2 nmol of Ca^{2+}/mg of SR protein dissociated from the protein, a number consistent with the number of high-affinity Ca^{2+} binding sites previously measured at equilibrium, in $^{45}Ca^{2+}$ filtration experiments, for our SR preparation (*25*,*37*).

The whole protocol relies on the fact (*29*) that quin2 binds Ca^{2+} very rapidly. Since this is a critical prerequisite, we checked it under our own conditions. Under the conditions of the experiment illustrated in Figure 1, i.e., at pH 7, 20 °C, 100 mM KCl, and in the absence of Mg^{2+}, we measured the rate constant for Ca^{2+} dissociation from the Ca^{2+}−quin2 complex, k_- [we found $k_- = 35$ s^{-1}, in agreement with results described in (*38*)], as well as the equilibrium dissociation constant for the complex, K_d [we found $K_d = 140$ nM (Table 1), in agreement with results described in (*29*)]. These numbers allowed us to calculate the bimolecular rate constant for Ca^{2+} binding to quin2, $k_+ = k_-/K_d$. This rate is $k_+ = 2.5 \times 10^8$ M^{-1} s^{-1} [see also (*39*)], in agreement with recent temperature-jump results (*40*). Thus, with a final free concentration of quin2 higher than, for instance, 40×10^{-6} M, the rate at which Ca^{2+} binds to quin2 (which is equal to k_+[quin2]) is faster than 10^4 s^{-1}, and the above prerequisite is fully satisfied. To excite quin2 fluorescence, we chose to use the mercury arc line at 313 nm of our Hg−Xe lamp, instead of the mercury arc line at 366 nm which was previously used (*28*), because the signal to noise ratio of the quin2 fluorescence changes is larger at 313 nm. The measured rate constants are identical at the two wavelengths (data not shown), but the amplitudes have opposite signs.

Comparison between $^{45}Ca^{2+}$ Binding and ATPase Intrinsic Fluorescence at Equilibrium

In the equilibrium measurements shown in Figure 6, to minimize nonspecific $^{45}Ca^{2+}$ binding to membranous sites different from the ATPase transport sites, we decided to use a medium containing 5 mM Mg^{2+} in addition to 100 mM KCl (under these conditions, the changes in Trp fluorescence are again faster than Ca^{2+} dissociation, as in the absence of Mg^{2+}; data not shown). To minimize background noise in $^{45}Ca^{2+}$ filtration measurements, we kept the total amount of $^{45}Ca^{2+}$ in the medium at a moderate level. We also minimized possible errors in the estimation of final free Ca^{2+} concentrations by using a low-affinity Ca^{2+} buffer, Mg−EDTA, for free Ca^{2+} concentrations in the micromolar range (*44*−*46*), as well as the commonly used EGTA for lower free Ca^{2+} concentrations. Identical samples were prepared for $^{45}Ca^{2+}$ binding and Trp fluorescence measurements as follows. To 11 mL aliquots of a solution containing 100 mM KCl, 5 mM Mg^{2+}, 50 mM Mops-Tris (pH 7, 20 °C), 20 μM $^{45}Ca^{2+}$, and 1 mM [^{3}H]glucose, we first added various amounts of either Mg−EDTA or EGTA (concentrations of Mg−EDTA ranged from 0.11 to 5.2 mM, resulting in final free Ca^{2+} concentrations from 10 to 0.3 μM, and concentrations of EGTA ranged from 0.045 to 2 mM, resulting in final free Ca^{2+} concentrations from 0.55 to below 0.005 μM), and then SR vesicles at a final concentration of 0.1 mg of protein/mL (assuming 5 μM contaminating and endogenous Ca^{2+}, the final total concentration of Ca^{2+} was therefore 25 μM). A few minutes later, on the one hand, 3 mL aliquots (in duplicate) were filtered on two superposed Millipore HA filters, to estimate the amount of bound $^{45}Ca^{2+}$ by double-label scintillation (squares); on the other hand, 2 mL aliquots were transferred into the fluorometer (again, in duplicate) and 4 μL of 1 M stock solution of EGTA was added to the fluorescence cuvette to measure the EGTA-induced drop in fluorescence (circles). For the fluorescence experiment, excitation and emission wavelengths were 290 and 345 nm, respectively; the emission slit was wide open (bw = 16 nm) to reduce the noise level to less than 0.1%, and the observed drop was corrected for the (very small) dilution-induced artefact. For the $^{45}Ca^{2+}$ binding measurement, the second filter, which has no adsorbed SR, served as a convenient control for the subtraction procedure involved in the double label counting (*47*); the error turned out to be less than 0.1 nmol/mg.

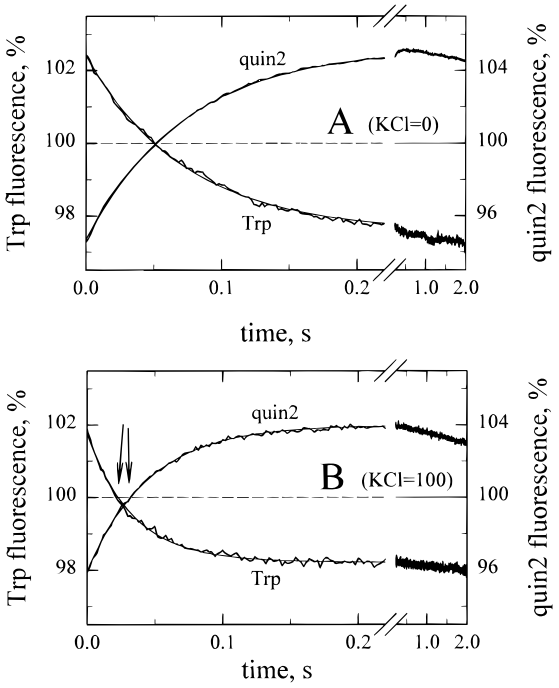

FIGURE 2: quin2 and Trp fluorescence changes in the absence (panel A) or presence (panel B) of KCl at neutral pH. SR vesicles (0.4 mg of protein/mL) were mixed one to one with 400 μM quin2 in a Biologic SFM-3 system, and we monitored successively quin2 fluorescence and Trp fluorescence. The excitation beam had a narrow spectral bandwidth (less than 1 nm). For quin2, λ_{ex} was 313 nm, and emitted light was detected through a wide-band filter (MTO DA531) centered at 530 nm. For Trp, λ_{ex} was 290 nm, and a combination of emission filters (MTO J324+A340) resulted in wide-band detection centered at 350 nm. The medium contained either 150 mM Mops-Tris (panel A) or 100 mM KCl and 50 mM Mops-Tris (panel B), at pH 6.9 and 24 °C in both cases; contaminating Ca^{2+} was sufficient to initially saturate the ATPase high-affinity sites. Similar results were obtained if 100 μM quin2 was used instead of 400 μM (not shown). The data were fitted to single exponentials, with observed rate constants for quin2 and Trp of 13.5 and 13.8 s^{-1}, respectively, in panel A and 21.7 and 30.4 s^{-1} in panel B; fits superimposed on the experimental data. Fluorescence levels have been plotted as % of their value at the halftime of the fit; the 100% line has been drawn (dashed line) to visualize the halftime for each trace (arrows in panel B).

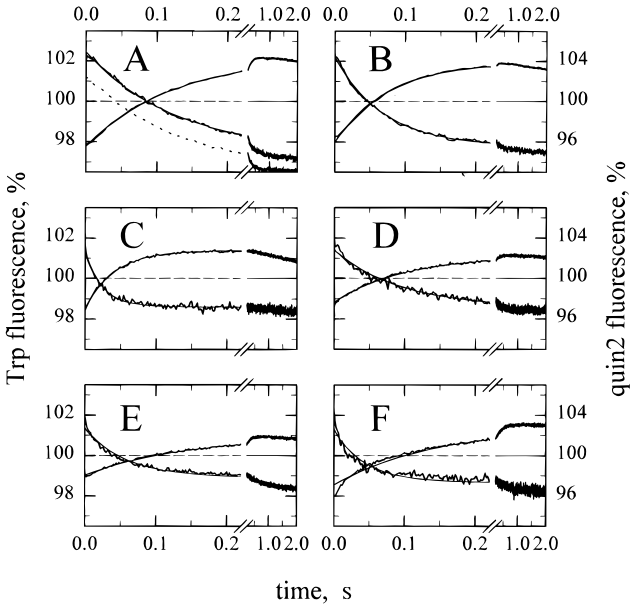

FIGURE 3: quin2 and Trp fluorescence changes under various ionic conditions. These experiments were performed at 24 °C as described for Figure 2, but under different ionic conditions. (Panels A and B) The medium contained either 150 mM Mes-Tris (panel A) or 100 mM KCl and 50 mM Mes-Tris (panel B) at pH 6, with an additional 10 μM Ca^{2+} in the SR syringe to ensure initial saturation of the ATPase Ca^{2+} binding sites. The dotted line in panel A shows a recording of Trp fluorescence in which 10 mM EGTA instead of 400 μM quin2 was used to trigger dissociation of Ca^{2+}. (Panels C−F) The medium contained either 250 mM KCl and 50 mM Mops-Tris at pH 6.9 (panel C), or 20 mM Mg^{2+} and 150 mM Mops-Tris at pH 6.9 (panel D), or 40 mM Mg^{2+} and 150 mM Mops-Tris at pH 7.25, i.e., conditions similar to those in (*19*) (panel E), or 150 mM Tes-Tris alone at pH 8.5 (panel F). The single exponentials which fit the data best are superimposed on the experimental data. Their rate constants are 8.04 and 8.0 s^{-1} in panel A; 12.9 and 14.3 s^{-1} in panel B; 23 and 42 s^{-1} in panel C; 9.7 and 10.8 s^{-1} in panel D; 6.95 and 17.7 s^{-1} in panel E; and 6.9 and 23 s^{-1} in panel F, for quin2 and Trp data, respectively (for panels D−F, single exponentials obviously provide a poor or very poor fit). Fluorescence levels have been plotted as % of their value at the halftime of the fitted curve.

RESULTS

Ca^{2+} Dissociation from SR Ca^{2+}-ATPase and Changes in ATPase Intrinsic Fluorescence, As Measured in the Presence of quin2: Effects of K^+ and pH

Figure 2 illustrates a stopped-flow experiment where Ca^{2+} dissociation from SR Ca^{2+}-ATPase was triggered by addition of quin2 at a concentration high enough to reduce free Ca^{2+} to less than 10^{-8} M. By selecting appropriate excitation wavelengths and emission filters for fluorescence detection, we were able to monitor quin2 fluorescence (i.e., Ca^{2+} dissociation) and the concomitant changes in tryptophan (Trp) fluorescence successively, under exactly the same ionic conditions. In the presence of 150 mM Mops-Tris and the absence of KCl, at pH 6.9 and 24 °C (panel A), quin2 and Trp fluorescence changes are both monoexponential, and there is impressive matching of halftimes for the Trp and quin2 fluorescence changes. Similar agreement between the results of stopped-flow Trp fluorescence measurements and those of rapid filtration measurements with $^{45}Ca^{2+}$ has been previously obtained in experiments performed in the absence of KCl (*19*,*25*), and this validates our use of quin2 for the same purpose. Figure 2B shows that this agreement is no longer observed when the experiment is repeated at the same pH but in the presence of 100 mM KCl (and only 50 mM Mops-Tris). In this case, the halftime for the changes in Trp fluorescence is distinctly shorter than that for Ca^{2+} dissociation. A similar difference beween the apparent halftimes for quin2 and Trp fluorescence changes in the presence of KCl at neutral pH is observed irrespective of the tested temperature, between 10 and 30 °C (data not shown).

Similar experiments were repeated under various ionic conditions (Figure 3). While at pH 6.9 in the presence of 100 mM KCl, the ratio of the rate constants for the Trp and quin2 fluorescence changes is 1.4 (Figure 2B), compared to 1.02 in the absence of KCl (Figure 2A), it increases to 1.8 in the presence of 250 mM KCl (Figure 3C). At neutral pH, the apparent effect of K^+ on the rate of the Trp fluorescence changes (*26*,*27*) is in fact larger than its effect on the rate of Ca^{2+} dissociation. At neutral pH (Figures 2 and 3C) as well as at acidic pH (Figure 3A and B), KCl only enhances the rate of the rise in quin2 fluorescence to a modest extent, consistent with the modest acceleration of $^{45}Ca^{2+}$ dissociation by K^+ that we previously found at pH 6 in rapid filtration experiments (*25*). At acidic pH, the

difference between Trp and quin2 traces in the presence of KCl is less prominent than at neutral pH, but it is still there (see also below): at pH 6, the ratio of rate constants is 1.11 (±0.01) in the presence of 100 mM KCl (see also below) and 1.00 (±0.01) in its absence (Figure 3A and B). The inclusion of 20 mM Mg^{2+} in the medium, at pH 6.9 in the absence of KCl, does not induce a drastic difference between the halftimes for quin2 and Trp fluorescence changes (panel D in Figure 3). However, Mg^{2+} becomes more efficient if the medium is made slightly more alkaline (panel E), and making the medium very alkaline in the absence of Mg^{2+} results in even larger discrepancies between the Trp and the quin2 traces (panel F). Together with KCl, pH is therefore a critical factor in permitting kinetic discrimination between Ca^{2+} dissociation and the accompanying Trp fluorescence changes. Panels D−F in Figure 3 also confirm that, under certain ionic conditions, the drop in Trp fluorescence significantly departs from monoexponential behavior, in agreement with previous results (*19*).

Dependence on the Excitation Wavelength of the Apparent Kinetics of the Changes in ATPase Intrinsic Fluorescence Accompanying Ca^{2+} Dissociation

We then found that the kinetics of the changes in ATPase Trp fluorescence depend to a significant extent on the wavelength used for excitation of these Trp residues. This dependence on the excitation wavelength can be observed in simple experiments (similar to the one illustrated in Figure 2B) in which 10 mM EGTA instead of 400 μM quin2 is used to trigger Ca^{2+} dissociation from the ATPase. At pH 7 and 20 °C and in the presence of 100 mM KCl, as shown in panel A in Figure 4, the kinetics of the EGTA-induced drop in Trp fluorescence are indeed much faster when excitation is set at 296 nm instead of 280 nm: fits to single exponentials give observed rate constants of 69 and 25 s^{-1}, respectively. Results with $\lambda_{ex} = 290$ nm (see dotted trace in Figure 4A) are similar to those with 280 nm. Figure 4B shows that this dependence on the excitation wavelength of the kinetics of the observed fluorescence changes is practically absent when the experiment is repeated in the absence of KCl. Its occurrence is, however, not specific to the presence of KCl, since it is even more clearly observed in the presence of NaCl (Figure 4C). In this case, the observed changes in fluorescence clearly comprise two phases of opposite sign when observed with $\lambda_{ex} = 296$ nm. The likely existence of a similar although less obvious second phase of opposite sign can in fact also be recognized in the trace obtained in the presence of KCl with 296 nm as the excitation wavelength (Figure 4A). Similar results are obtained when the experiment is performed in the presence of quin2 instead of EGTA (data not shown).

This wavelength dependence of the response of ATPase Trp fluorescence presumably arises because the various Trp residues in ATPase do not all respond to Ca^{2+} dissociation in the same way, and some of them are optically selected when a long excitation wavelength is used (see below). However, this dependence is also responsible for the difference between the standard results shown above in Figure 2 and those, now illustrated in Figure 5, obtained when a broader spectral bandwidth for the excitation beam is used in conjunction with the same nominal excitation wavelength of 290 nm. In the latter case, under comparable if not identical conditions, the apparent discrepancy between Trp

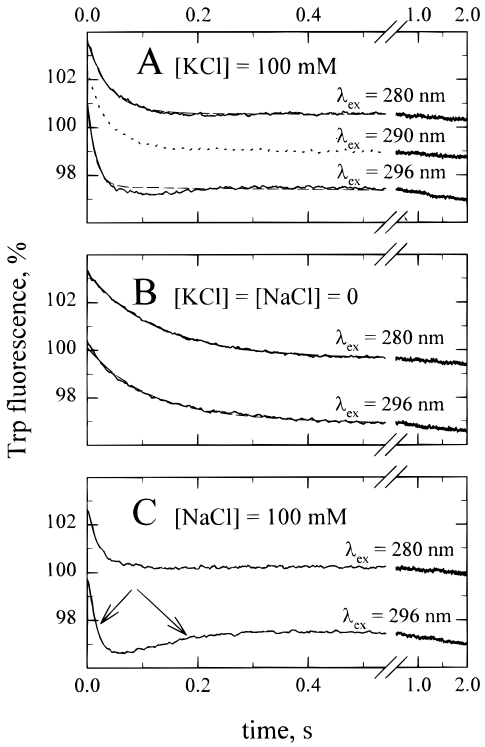

FIGURE 4: Dependence on the excitation wavelength of the apparent kinetics of EGTA-induced Trp fluorescence changes at pH 7 under various ionic conditions. These experiments were performed with the Biologic SFM-3 system and a narrow spectral bandwidth (less than 1 nm) for the excitation beam, using different wavelengths for excitation of Trp fluorescence, as indicated. SR vesicles at 0.4 mg/mL, to which 100 μM Ca^{2+} had been added, were mixed one to one with 10 mM EGTA. The medium was buffered at pH 7 and 20 °C, and contained 100 mM KCl and 50 mM Mops-Tris (panel A), 150 mM Mops-Tris and no KCl (panel B), or 100 mM NaCl and 50 mM Mops-Tris (panel C). When the data in panels A and B are fitted to single exponentials, the following rate constants are found: in panel A, 23 s^{-1} (280 nm), 25 s^{-1} (290 nm), and 65 s^{-1} (296 nm); in panel B, 8.0 s^{-1} (280 nm) and 9.0 s^{-1} (296 nm).

and quin2 traces in the presence of KCl (Figure 5B) is larger than in Figure 2B, with a ratio for the rate constants of Trp and quin2 fluorescence changes at pH 7 of 3 in Figure 5B, instead of 1.4 in Figure 2B. At pH 6 (data not shown) in the presence of KCl, this ratio of rate constants for Trp and quin2 fluorescence changes is 1.6 (instead of 1.1 in Figure 3B), whereas in the absence of KCl it is 1.03 (instead of 1.00 in Figure 3A). The apparent discrepancy, when it exists, between Trp traces and quin2 traces is therefore larger when Trp fluorescence is excited with the broader spectral bandwidth. The main reason for this difference is the presence, in the emission spectrum of the mercury-doped xenon lamp used for excitation, of a sharp and intense mercury arc line at 296/297 nm, superimposed on the relatively broad spectrum characteristic of xenon: combining a nominal excitation wavelength of 290 nm with a spectral bandwidth that is too broad therefore results in an excitation beam which is in fact dominated by the arc line at 296/297 nm (this also accounts for the smaller relative amplitudes of the fluorescence changes in Figure 5 compared to Figure 2).

Significance of Trp Fluorescence Levels at Equilibrium and Optical Selection of Specific Trp Residues

We finally wondered whether the fact, observed in time-resolved experiments, that rapid dissociation of the first Ca^{2+}

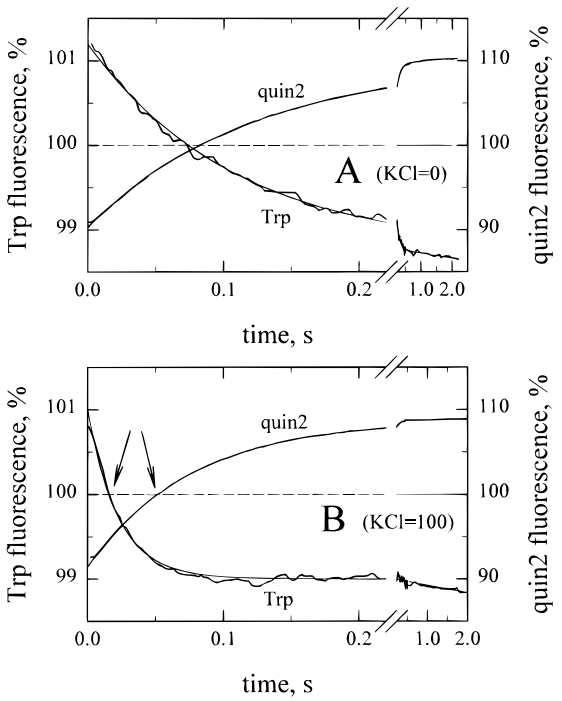

FIGURE 5: quin2 and Trp fluorescence changes in the absence (panel A) or presence (panel B) of KCl at pH 7, as observed with a wide spectral bandwidth for excitation. This experiment is similar to that shown in Figure 2, except for a few differences. Here, SR vesicles were mixed one to one with 100 μM quin2, and the medium was buffered at pH 7 and 20 °C. This experiment was performed with a Dionex 110 instrument in which the observation chamber had an optical pathlength of 20 mm (hence the lower concentration of quin2, to avoid inner filter problems) and was illuminated at a nominal wavelength of 290 nm but with a broad spectral bandwidth (about 4 nm). The data were fitted to single exponentials, with observed rate constants for quin2 and Trp fluorescence of 8.4 and 9.2 s^{-1}, respectively, in panel A and 14 and 44 s^{-1} in panel B.

ion apparently plays a dominant role in Trp fluorescence changes in the presence of KCl has any counterpart in experiments performed at equilibrium. The answer is yes. Figure 6 first shows an experiment which was designed to compare, at various pCa values under equilibrium conditions at pH 7, the amount of $^{45}Ca^{2+}$ bound to the ATPase (squares) with the ATPase intrinsic fluorescence, excited at 290 nm (in fact, the circles correspond to the relative *difference* between this level, at the indicated pCa value, and the level of the same sample after addition of EGTA). Care was taken to minimize possible sources of error (see Experimental Procedures). The logarithmic *Y* scale in Figure 6 makes it clear that squares and circles are *not* superimposed at low Ca^{2+} concentrations: bound $^{45}Ca^{2+}$ reaches 10% of its maximal value (see horizontal dotted line; this corresponds to a level that we could measure reliably) at a concentration of free Ca^{2+} for which the Trp fluorescence has not yet risen to a significant extent; and when the Trp fluorescence signal reaches 10% of its own maximal value, bound $^{45}Ca^{2+}$ is proportionally much larger. The Ca^{2+}-dependent rise in Trp fluorescence exhibits a higher index of positive cooperativity ($n_H = 1.6$) and a higher $Ca_{0.5}$ than $^{45}Ca^{2+}$ binding, the positive cooperativity of which is poorer ($n_H = 1.3$). Thus these results show that at equilibrium in the presence of KCl the intrinsic fluorescence level of Ca^{2+}-ATPase does not exactly parallel $^{45}Ca^{2+}$ binding but exhibits a dependence on free Ca^{2+} which has a slightly larger positive cooperativity, as if Trp fluorescence—even when excited at 290 nm—were

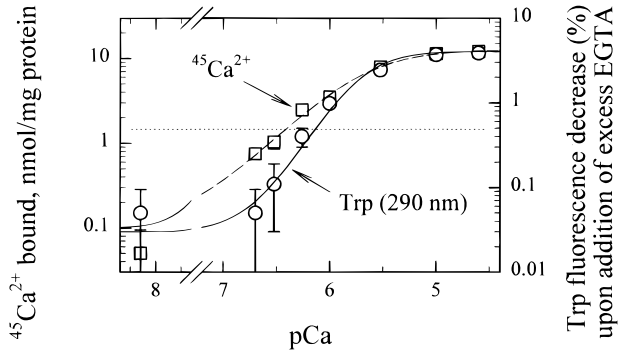

FIGURE 6: Comparison between ATPase Trp fluorescence and $^{45}Ca^{2+}$ bound at equilibrium. Squares show the dependence on pCa of the amount of $^{45}Ca^{2+}$ bound at equilibrium to the ATPase high-affinity sites. Circles show the *difference* between the fluorescence of ATPase at the indicated pCa and that of Ca^{2+}-free ATPase, obtained after addition of excess EGTA; this difference is expressed in %, relative to ATPase fluorescence. Identical SR samples were prepared for the $^{45}Ca^{2+}$ binding measurements and for the Trp fluorescence measurements, both performed in duplicate in a medium containing 5 mM Mg^{2+}, 100 mM KCl, and 50 mM Mops-Tris at pH 7 and 20 °C (see Experimental Procedures). Unless indicated by an error bar, the difference between duplicates was smaller than the size of the symbols. The dotted horizontal line represents 12% of the maximal signal, the latter being a 4% change for Trp fluorescence and 12 nmol/mg of protein for bound $^{45}Ca^{2+}$ (note the different log scales on the *Y* axis for $^{45}Ca^{2+}$ and Trp data). Lines through data points correspond to fits with $K_d = 2.0$ μM and $n_H = 1.3$ ($^{45}Ca^{2+}$ data) and $K_d = 2.3$ μM and $n_H = 1.6$ (Trp data).

especially sensitive to binding of the second Ca^{2+} ion (i.e., the first ion to leave, in dissociation experiments).

We then examined the effect of the excitation wavelength on equilibrium fluorescence levels (Figure 7). We found that when ATPase fluorescence is excited at 300 nm instead of 280 nm, the emission spectrum is in fact shifted toward longer wavelengths by about 2 nm (panel A in Figure 7, dotted line versus continuous line, see asterisk). Excitation spectra provide the same information (panel B, dotted line versus continuous line, see asterisk at the red edge of the excitation spectrum). Consequently, we examined Ca^{2+}-dependent changes in ATPase fluorescence with two different combinations of excitation *and* emission wavelengths (panel C in Figure 7). In both cases, the initial addition of EGTA to SR vesicles (previously equilibrated with contaminating Ca^{2+} in a medium containing 100 mM NaCl and 50 mM Mops-Tris at pH 7—a medium chosen to maximize the anticipated differences) resulted in a large drop in fluorescence. This was followed by several additions of Ca^{2+}, to progressively increase the free Ca^{2+} concentration up to saturation. The experiment illustrated by the top trace in Figure 7C, recorded with $\lambda_{ex} = 280$ nm and $\lambda_{em} = 320$ nm, displays the usually observed progressive Ca^{2+}-dependent rise in ATPase intrinsic fluorescence. However, the bottom trace, recorded with $\lambda_{ex} = 302$ nm and $\lambda_{em} = 350$ nm, displays a slightly different pattern: with these longer excitation and emission wavelengths, the first addition of Ca^{2+}, which presumably favors the formation of ATPase species with only one Ca^{2+} ion bound, results in a small *drop* (instead of a rise) in ATPase fluorescence; subsequent additions of Ca^{2+} revert this drop, but after the third addition of Ca^{2+}, i.e., at pCa 5.7, the ATPase fluorescence level is still significantly different from its maximum (as shown by the relatively large effect of the fourth addition) whereas at pCa 5.7 an almost maximal fluorescence level has already

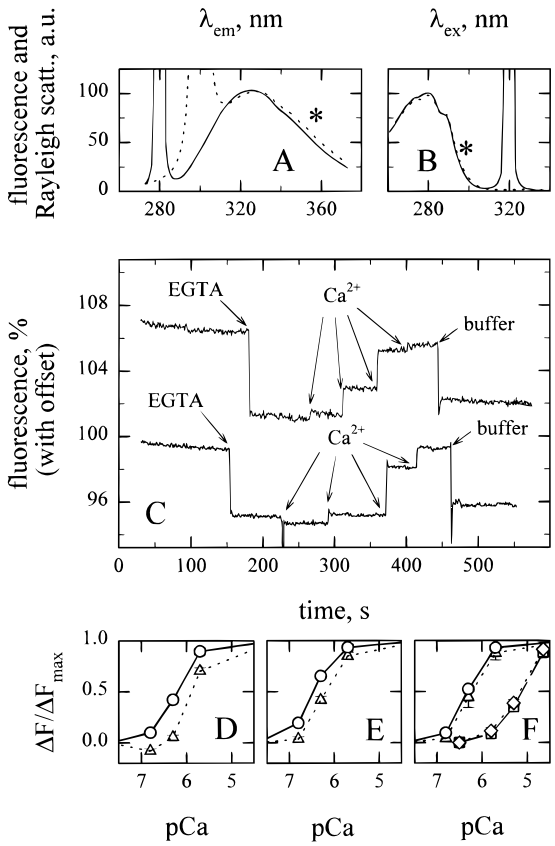

FIGURE 7: Ca^{2+}-dependence of ATPase intrinsic fluorescence depends on which Trp residues are optically selected. SR vesicles (0.1 mg of protein/mL) were suspended in 2 mL of a medium containing either 100 mM KCl and 50 mM Mops-Tris at pH 7 and 20 °C (panels A, B, and E), or 100 mM NaCl and 50 mM Mops-Tris at pH 7 (panels C and D), or neither KCl nor NaCl but either 150 mM Mops-Tris at pH 7 (circles and triangles in panel F) or 150 mM Mes-Tris at pH 6 (squares and diamonds in panel F). (Panel A) Fluorescence emission spectra, with either $\lambda_{ex} = 280$ nm (continuous line) or $\lambda_{ex} = 300$ nm (dotted line) (bw = 2 nm). Raman scattering was subtracted, and spectra were normalized and plotted in arbitrary units au. (Panel B) Excitation spectra, with either $\lambda_{em} = 320$ nm (continuous line) or $\lambda_{em} = 370$ nm (dotted line). Asterisks point to small red shifts. (Panel C) Ca^{2+}-dependent changes in ATPase intrinsic fluorescence. Traces were recorded either with $\lambda_{ex} = 280$ nm and $\lambda_{em} = 320$ nm (top trace) (1 and 10 nm bw, respectively) or with $\lambda_{ex} = 302$ nm and $\lambda_{em} = 350$ nm (bottom trace) (5 and 10 nm bw, respectively), and were shifted with respect to each other by a few % offset. In both cases, 4 μL of EGTA (0.5 M stock solution) was first added, followed by four additions of Ca^{2+}, 2.2 μL each (0.25 M stock solution); pCa after each addition was 6.8, 6.3, 5.7, and 4.0, respectively. The artefacts due to dilution have not been corrected for, but they are very small for these additions. Finally, 80 μL of buffer was added as a control, resulting in 4% dilution of the sample. (Panels D−F) pCa-dependence of the normalized fluorescence changes in different media, using either lower (circles and squares) or higher (triangles and diamonds) excitation and emission wavelengths, as for panel C; each data point is the mean ± SD of 2−4 measurements.

been reached at the shorter wavelength (as shown by the very small effect of the fourth addition in the top trace of panel C). The pCa-dependence of these fluorescence changes is plotted in Figure 7D: it is shifted to higher Ca^{2+} concentrations at long wavelengths (triangles) compared to short wavelengths (circles).

Similar experiments were performed under other ionic conditions. In the presence of KCl instead of NaCl (panel E in Figure 7), although the intermediate free Ca^{2+} concentrations at which ATPase has a reduced fluorescence are not clearly resolved, the free Ca^{2+} concentration for which fluorescence finally rises is still unambiguously shifted to a higher value, as in the presence of NaCl, when fluorescence is excited at the longer wavelength (triangles versus circles in panel E). In contrast, in the absence of KCl or NaCl, there is almost no difference between the results collected at long or short wavelength at pH 7 (triangles or circles in Figure 7F), and at pH 6 there is none at all (diamonds or squares in Figure 7F); at this pH, the affinity of Ca^{2+} binding to the ATPase shifts to higher Ca^{2+} concentrations, as previously noted (*37*). These results concerning the wavelength-dependence under various ionic conditions of the pCa-dependence of ATPase fluorescence are consistent with our time-resolved results in Figure 4. Together with the equilibrium results in Figure 6, they also demonstrate that at neutral pH in the presence of KCl or NaCl, the apparent positive cooperativity with which Ca^{2+} binds to Ca^{2+}-ATPase is not very high. If it were high, the ATPase would exist almost exclusively either as the Ca^{2+}-free species or as the species with two Ca^{2+} ions bound, and all spectroscopic properties would have the same pCa-dependence, which is not the case in Figures 7D and 7E. In contrast, if Ca^{2+} binds with poor positive cooperativity, significant amounts of ATPase species with only one Ca^{2+} ion bound may accumulate at intermediate Ca^{2+} concentrations, with their own specific spectroscopic properties; thus changes at different excitation (and emission) wavelengths may have different pCa-dependences because they may be dominated by any one of the three main ATPase intermediates [see a similar rationale about binding of Sr^{2+}, a Ca^{2+} analog, in (*48*,*49*)].

DISCUSSION

Use of quin2 To Compare the Rate of Ca^{2+} Dissociation from Ca^{2+}-ATPase with the Accompanying Trp Fluorescence Changes

We show here that quin2 can be successfully used to measure, under exactly the same conditions, the kinetics of Ca^{2+} dissociation from Ca^{2+}-ATPase and the accompanying changes in ATPase intrinsic fluorescence. The Trp fluorescence kinetics measured in the presence of quin2 are identical to those measured in more conventional experiments in the presence of EGTA (e.g., see Figure 3A), which shows that absorbance of quin2 in the UV region (*29*) is not an obstacle to these measurements (especially if an optical cell with a short pathlength is used). To our knowledge, combining Trp fluorescence measurements with quin2 fluorescence measurements in this way had never been attempted before, presumably because most of the small soluble Ca^{2+}-binding proteins for which this quin2 technique was developed (*28*) have no Trp residues to be studied. As previously deduced from comparison of Trp fluorescence measurements with a few $^{45}Ca^{2+}$ rapid filtration studies (*12*,*18*,*19*,*25*), our data confirm that under certain conditions the Trp fluorescence changes exactly parallel overall Ca^{2+} dissociation from the ATPase. However, this is not the case under all ionic conditions, especially in the presence of KCl or NaCl under otherwise standard conditions for pH, temperature, and Mg^{2+} (Figures 2−5). In particular, the true effect of KCl on the rate of Ca^{2+} dissociation is much more modest than its previously described effect (*19*,*26*) on the rate of Trp fluorescence changes.

Analysis of the Pseudo-Monophasic Kinetics of Ca^{2+} Dissociation

A remarkable result of our experiments is that under all of these neutral or acidic conditions, the kinetics of overall Ca^{2+} dissociation, as deduced from the changes in quin2 fluorescence, are fitted remarkably well by single exponentials (e.g., see Figures 1, 2, 3A−D, and 5, in which fits to single exponentials superimposed on the quin2 data are shown). This fact was previously noted in indirect or direct measurements of Ca^{2+} dissociation [phosphorylation measurements in (*24*); $^{45}Ca^{2+}$ filtration measurements in (*25*)], but the high signal to noise ratio in the present experiments makes this observation even more certain. Since dissociation of the two Ca^{2+} ions has been shown to be sequential (*12*,*13*,*23*−*25*), the pseudo-monophasic time course of overall Ca^{2+} dissociation places constraints on the models accounting for this dissociation (*25*). These constraints are not easily deduced from intuition only but can be obtained by solving the simple differential equations which govern evolution of the system: it turns out [Figure 1 in (*50*)] that for sequential dissociation to result in an apparently monoexponential loss of Ca^{2+} from the ATPase, the ratio between the rate constants (k_1 and k_2) for dissociation of the first and the second ions must be close to 2, and the rate constant for overall dissociation (k_{diss}) then corresponds to the rate constant for dissociation of the second ion. Figure 8A shows a simulation corresponding to this situation: the time-dependence of the various species during Ca^{2+} dissociation is shown by the continuous lines in Figure 8A, while the concomitant drop in bound Ca^{2+} is shown by the dashed line. Thus, a consequence of monophasic overall Ca^{2+} dissociation is that from this single measurement the rates of dissociation of the first and second Ca^{2+} ions can both be estimated.

Analysis of the Kinetics of Trp Fluorescence Changes, Using a Three-Species Model

These Ca^{2+} dissociation rates can then be used to simulate the expected kinetics of the Trp fluorescence changes. The latter depend on the exact fluorescence levels assumed for the various species. If we assume that the three-species model shown on top of Figure 8 correctly describes Ca^{2+}-ATPase, then if the fluorescence level of the ECa species is exactly between those of the ECa_2 and E species, the changes in Trp fluorescence will exactly parallel overall Ca^{2+} dissociation and its mirror image, quin2 fluorescence (dashed lines in Figure 8B). According to this analysis, this seems to be the case in the absence of KCl (Figures 2A and 5A; see below, however). Alternatively, if the entire drop in ATPase fluorescence already occurs as the result of the dissociation of the first ion, the Trp fluorescence drop will be twice as fast as the overall rate of Ca^{2+} dissociation, since its time course will match that of the ECa_2 species (continuous lines in Figure 8 A and B). This seems to be almost the case at neutral pH in the presence of a high KCl concentration, when Trp fluorescence is excited at 290 nm (Figures 2B and 3C). We are thus tempted to conclude that under these conditions, changes in ATPase intrinsic fluorescence are mainly dominated by the dissociation kinetics of the first Ca^{2+} ion. We had previously reached a similar conclusion regarding the significance of the Trp fluorescence changes accompanying dissociation of Sr^{2+}, an analog of Ca^{2+} which

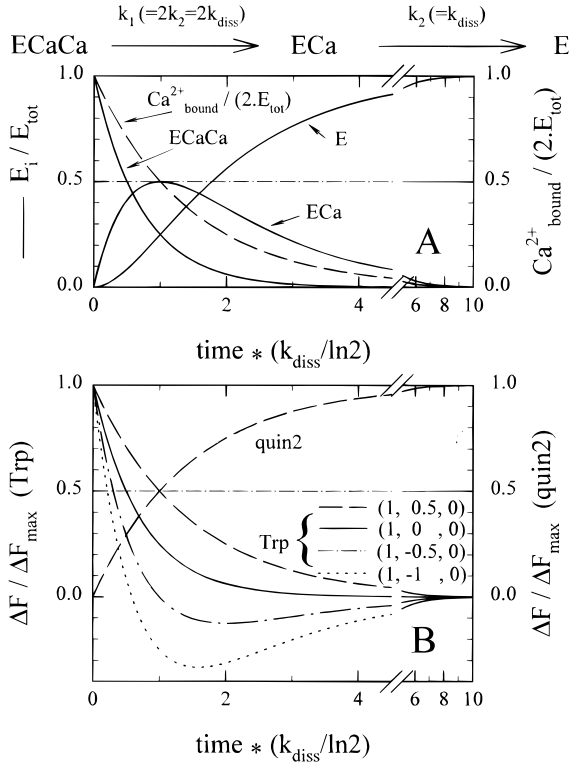

FIGURE 8: Theoretical simulation of possible responses of intrinsic fluorescence to sequential Ca^{2+} dissociation from the ATPase. (Top Scheme) Model with three species for sequential but monophasic Ca^{2+} dissociation. The species with only one Ca^{2+} ion might actually comprise a mixture of species in rapid equilibrium, with the single residual Ca^{2+} ion shuttling back and forth between a deeper and a more superficial position in the binding crevice (*25*); similarly, all Ca^{2+}-free species in rapid equilibrium are treated as a single species. (Panel A) Time-dependence after Ca^{2+} chelation of the relative concentrations of the various species (continuous lines) and of the residual amount of Ca^{2+} bound to the ATPase (dashed line). The scale for the abscissa is normalized to the half time for overall Ca^{2+} dissociation, (ln 2)/k_{diss}. (Panel B) Time-dependence of the drop in Trp fluorescence. This drop is a linear combination of the concentrations of the various species E_i, with coefficients depending on the relative fluorescence of each species; if fluorescence levels are written f_{Ei}, the coefficients are $(f_{Ei} - f_E)/(f_{ECaCa} - f_E)$. Four specific assumptions are considered, and the corresponding coefficients are indicated in the figure. When the fluorescence level of the intermediate species is lower than that of the final species (negative coefficient for ECa), an undershoot is observed. The expected rise in quin2 fluorescence, which reflects Ca^{2+} dissociation, is also indicated (dashed line upward).

binds to the same sites as Ca^{2+} but with a lower affinity (*49*).

At first sight, it seems that no spectroscopic event can occur with an apparent rate constant faster than the rate constant for dissociation of the first Ca^{2+} ion (i.e., $2k_{diss}$). However, if the intermediate ECa species has an overall Trp fluorescence level *lower* than that of the final species, the observed Trp signal in fact comprises both a fast drop and a subsequent slower rise (in Figure 8B, the dotted line and the dashed-dotted line illustrate two such *cases*). Depending on the assumed fluorescence levels, the slower rise may be only poorly apparent (e.g., the simulated dashed-dotted line in Figure 8B), and in experimental data, it may be even less apparent, because of noise level and on-going photolysis (see Figure 5B or 4A, where Trp fluorescence changes in the presence of KCl are observed either with a nominal wavelength of 290 nm but with a Hg−Xe lamp and a broad spectral bandwidth for excitation or with an excitation

wavelength of 296 nm). If in such cases the second phase is overlooked and a single-exponential analysis is applied to the data (truly biphasic, with amplitudes of opposite sign), the outcome of this analysis is an *apparent* halftime shorter than that of the dissociation of the first Ca^{2+} ion: the unduly short halftime deduced from such naïve single-exponential analysis simply reflects the existence of intermediate species with an overall fluorescence lower than that of the final species. The existence of these ATPase intermediate species with low fluorescence is of course made even clearer by the unambiguous undershoot observed in the presence of NaCl when a long excitation wavelength is used (Figure 4C).

Analysis of Trp Fluorescence Changes, Using a Four-Species Model: Conformational Changes of Ca^{2+}-Free ATPase and the Effect of K^+ or Na^+

The fact that, in the presence of K^+ or Na^+, intermediate ATPase species presumably with only one Ca^{2+} ion bound have an overall fluorescence level lower than or similar to (depending on the excitation wavelength) that of the Ca^{2+}-deprived E species then raises the question of why, in the absence of K^+ or Na^+, the kinetics for Trp fluorescence changes and for overall Ca^{2+} dissociation are found to be similar. This question can be answered by accepting that the three-species model for dissociation shown on Figure 8 (and reproduced below as Scheme 1) is an oversimplification, and that more realistic models (e.g., Scheme 2 below, as in (*2*)) must comprise an equilibrium between different conformations of Ca^{2+}-free ATPase:

Scheme 1

$$ECa2 - ECa - E$$

Scheme 2

$$E1Ca2 - E1Ca - E1 - E2$$

Scheme 2 can indeed account for the results obtained both in the presence *and* the absence of monovalent cations if (i) the equilibrium between E1 and E2 favors E1 in the presence of monovalent ions *but shifts toward E2 in their absence*, as in fact previously suggested (*27*), (ii) the relative fluorescence level of the newly introduced E2 species is even lower than that of the E1Ca species, while that of E1 is higher than that of E1Ca, and (iii) transitions between E1 and E2 are fast compared with the Ca^{2+} dissociation steps, especially in the absence of monovalent cations. Hypotheses i and ii imply that the average fluorescence level of Ca^{2+}-deprived ATPase (the equivalent E species depicted in the simpler Scheme 1) is lower than that of E1Ca in the absence of monovalent cations but may be equal to it or even higher in their presence. In agreement with this, in experiments performed at pH 7 and in the absence of Mg^{2+}, we found that in the presence of Ca^{2+}, the ATPase fluorescence level is the same in the absence or presence of 100 mM K^+, whereas in the absence of Ca^{2+}, it is lower in the absence of K^+ [Champeil and Guillain, unpublished data; see also Figure 8 in (*27*)]. Hypothesis iii is required to account for the fact that Trp fluorescence drops fit reasonably well to single-exponential processes in the absence of monovalent cations. A very simple mechanism for the nonspecific effect of monovalent cations on the E1/E2 equilibrium of Ca^{2+}-ATPase suggested by hypothesis i would be competition with protons (*27*): monovalent cations (especially Na^+, which is closer to H^+) could bind to some of the sites for protons on E1 but prevent the previously recognized proton-induced shift from E1 to E2 (*37*,*51*−*53*). This antagonistic effect of monovalent cations in favor of E1 might also be part of the reason why, in Ca^{2+}-ATPase, phosphorylation from inorganic phosphate (believed to occur on the E2 form) is reduced in the presence of KCl and NaCl [e.g., (*54*)]; of course, part of this reduction is also due to acceleration of ATPase dephosphorylation [e.g. (*55*)].

In structural terms, if the E2 conformation is significantly different from E1, with long-range reorganization extending up to the ATPase phosphorylation site, it is not surprising that this delocalized change also affects the exact fluorescence level of the various Trp residues in ATPase; the fluorescence level would then be altered *both* upon Ca^{2+} binding or dissociation *and* upon changing conformation, a possibility at slight variance with the simpler versions previously proposed, which considered hypotheses in which fluorescence changes occurred *either* as a result of Ca^{2+} binding *or* as a result of conformational changes [e.g. (*53*)].

These different putative conformations of Ca^{2+}-free ATPase have been the subject of much controversy over the years [e.g. (*16*,*56*)]. Examining the various intermediates formed during Ca^{2+} dissociation in more detail is not possible here, since we need an additional and different index of the ATPase conformational state. However, the well-known FITC probe, specifically bound to lysine515 in the ATPase cytoplasmic domain, might be useful for providing such an index. We previously showed that it is possible to monitor both Trp fluorescence and FITC fluorescence changes with an FITC-labeled enzyme (*49*,*57*), and in the present work we show that it is also possible to monitor Ca^{2+} dissociation from such an FITC-labeled ATPase with quin2 (for instance, the SR vesicles which were used for the particular experiment illustrated in Figure 1 were FITC-labeled SR vesicles). Thus, the present work provides a starting point for future comparison between Trp fluorescence changes, FITC fluorescence changes and Ca^{2+} dissociation from FITC-labeled Ca^{2+}-ATPase under exactly the same ionic conditions.

Cooperativity of Equilibrium Ca^{2+} Binding to ATPase

Under equilibrium conditions at neutral pH and in the presence of monovalent cations, various parameters reflecting Ca^{2+} complexation with the ATPase do not all display exactly the same Ca^{2+}-dependence: the Ca^{2+}-dependence of the amount of ATPase-bound $^{45}Ca^{2+}$ is less cooperative than that of the accompanying Trp fluorescence (Figure 6), and Trp fluorescence changes do not have exactly the same midpoint if they are observed with shorter or longer excitation wavelengths (Figure 7C−E). Irrespective of the detailed mechanism, this implies that ATPase species, intermediate in the reaction sequence between Ca^{2+}-saturated ATPase and Ca^{2+}-deprived ATPase and with specific fluorescence properties, exist at equilibrium in significant amounts: this implies that the cooperativity for binding of the two Ca^{2+} ions is not very high. Analyzing $^{45}Ca^{2+}$ binding experiments performed in the absence of monovalent cations, Forge et al. previously found that the Hill index for $^{45}Ca^{2+}$ binding is high under acidic conditions but is significantly lower under alkaline conditions (*37*). In agreement with this, we find that Trp fluorescence changes observed with shorter

and longer excitation wavelengths no longer differ in their Ca^{2+} dependence when the experiment is performed at acidic pH (Figure 7F). Our results therefore support the conclusions of Forge et al. and provide an independent test that under selected conditions Ca^{2+} binding cooperativity may be rather low. They also suggest that at pH 7, K^+ and Na^+ ions make Ca^{2+} binding even less cooperative (Figure 7F), presumably because of a shift in the pH-dependent equilibrium (Scheme 2) preceding Ca^{2+} binding (or following Ca^{2+} dissociation). The question arises of whether Ca^{2+} binding to E1 has any cooperativity at all per se: the putative E1/E2 pre-equilibrium was theoretically shown long ago to have the capacity for imposing various degrees of cooperativity (*58*). In this view, Sr^{2+}, the Ca^{2+} analog (*48*,*49*), would only differ from Ca^{2+} because of its different affinity for Ca^{2+}-ATPase and not because of any difference in the cooperativity of intrinsic binding. This is presently under examination.

Optical Selection of Trp Residues Especially Sensitive to Ca^{2+} Dissociation

Finally, it is worth discussing the dependence on excitation wavelength of the kinetics of the changes in ATPase Trp fluorescence observed upon dissociation of Ca^{2+}. This up-to-now unsuspected dependence explains why a very large effect of K^+ on the rate of Trp fluorescence changes was reported in (*26*), since for Trp fluorescence excitation the authors used the 296/297 nm mercury arc line of their lamp. On the other hand, a relatively large effect of K^+ on EGTA-induced fluorescence changes was also reported in (*19*)*; in this case,* the nominal excitation wavelength was 290 nm but might have been contaminated with 296/297 nm light, as was the case in our own experiments with a broad band setup (Figure 5B). This dependence on excitation wavelength reflects optical selection of different subpopulations of Trp residues in the ATPase [13 Trp residues; see (*59*)], presumably with slightly different spectroscopic properties. The idea that Trp residues in ATPase do not constitute a homogenous population is warranted by a number of selective quenching experiments [see (*60*) and references therein]. Certain residues could dominate fluorescence upon excitation at short wavelengths. It is possible also that at short excitation wavelengths, Trp residues could experience intramolecular energy transfer from nearby tyrosine (or other Trp) residues, and the fluorescence signal observed would then reflect space-averaged changes around these residues (*61*). At long excitation wavelengths, the probability of such transfer is anyway reduced and the fluorescence signal certainly reflects the contribution of selected Trp residues, preferentially excited at this wavelength (and also emitting at slightly longer wavelength, as suggested by Figure 7A).

These residues behave in a remarkable way, since when excited at long wavelength in the presence of KCl or NaCl, they respond by fluorescence changes of opposite sign to dissociation of the first and the second Ca^{2+} ions, as shown in Figure 4A and C (or to binding of the first and the second Ca^{2+} ions, as shown in Figure 7C and D). These results are reminiscent of the results of two previous investigations in which ATPase in a somewhat modified environment was found to bind only one Ca^{2+} ion with a high-affinity and simultaneously to exhibit a *drop* in Trp fluorescence upon binding of this single Ca^{2+} ion, whereas unperturbed ATPase normally exhibits a *increase* in fluorescence upon binding of two Ca^{2+} ions. This unusual situation occurred when Ca^{2+}-ATPase was reconstituted in the presence of short-chain lipids (*62*,*63*) or when membranous ATPase was perturbed by the non-ionic detergent dodecyl maltoside (*64*,*65*). We can now conclude that in these previous studies the ability of Trp residues to exhibit reduced fluorescence under conditions resulting in formation of ATPase species with only one Ca^{2+} ion bound was not simply the result of ATPase perturbation, since specific Trp residues in *native* ATPase also respond by a rise in fluorescence to the dissociation of the second Ca^{2+} ion (Figure 4A and C, and Figure 7C and D). This second ion is presumably the one bound to the "deeper" site, which remains relatively unaltered in the presence of either short-chain phospholipids or dodecyl maltoside, despite the loss of the more superficial site. If certain Trp residues mainly respond to dissociation of the first Ca^{2+} ion by a drop in fluorescence, whereas others mainly respond to dissociation of the second Ca^{2+} ion by a rise in fluorescence, then future mutation of the various Trp residues in Ca^{2+}-ATPase, coupled with the spectroscopic characterization suggested here, might allow recognition of the residues especially sensitive to Ca^{2+} dissociation from one or the other of these two high-affinity transport sites.

ACKNOWLEDGMENT

We thank S. Orlowski for his initial contribution to the results shown in Figure 6 and for his continued interest, L. Combettes, B. Berthon, and M. Claret for introducing us to the beauties of quin2 fluorescence, F. Guillain for his assistance with the stopped-flow equipment and for discussion of the manuscript, E. Mintz, V. Forge, M. le Maire, and J. Sturgis for also commenting on the manuscript, and A. W. Boyd for his assistance in editing it.

REFERENCES

1. Hasselbach, W. (1974) in *The Enzymes* (Boyer, P. D., Ed.) 3rd ed., pp 432−467, Academic Press, New York.
2. de Meis, L., and Vianna, A. L. (1979) *Annu. Rev. Biochem. 48*, 275−292.
3. Jencks, W. P. (1989) *J. Biol. Chem. 264*, 18855−18858.
4. Inesi, G., Lewis, D., Nikic, D., Hussain, A., and Kirtley, M. E. (1992) *Adv. Enzymol. Relat. Areas Mol. Biol. 65*, 185−215.
5. Champeil, P. (1996) in *Biomembranes* (Lee, A. G., Ed.) Vol. 5, pp 43−76, JAI Press Inc., Greenwich, CT.
6. Makinose, M. (1973) *FEBS Lett. 37*, 140−143.
7. Bigelow, D. J., and Inesi, I. (1992) *Biochim. Biophys. Acta 1113*, 323−338.
8. Dupont, Y. (1976) *Biochem. Biophys. Res. Commun. 71*, 544−550.
9. Dupont, Y., and Leigh, J. B. (1978) *Nature 273*, 396−398.
10. Guillain, F., Gingold, M. P., Büschlen, S., and Champeil, P. (1980) *J. Biol. Chem. 255*, 2072−2076.
11. Guillain, F., Champeil, P., Lacapère, J. J., and Gingold, M. P. (1981) *J. Biol. Chem. 256*, 6140−6147.
12. Dupont, Y. (1982) *Biochim. Biophys. Acta 688*, 75−87.
13. Dupont, Y. (1984) *Anal. Biochem. 142*, 505−510.
14. Ikemoto, N., Miyao, A., and Kurobe, Y. (1981) *J. Biol. Chem. 256*, 10809−10814.
15. Champeil, P., Gingold, M. P., Guillain, F., and Inesi, G. (1983) *J. Biol. Chem. 258*, 4453−4458.
16. Petithory, J. R., and Jencks, W. P. (1988b) *Biochemistry 27*, 8626−8635.
17. Wakabayashi, S., and Shigekawa, M. (1990) *Biochemistry 29*, 7309−7318.
18. Forge, V., Mintz, E., and Guillain, F. (1993b) *J. Biol. Chem. 268*, 10961−10968.
19. Henderson, I. M. J., Starling, A. P., Wictome, M., East, J. M., and Lee, A. G. (1994b) *Biochem. J. 297*, 625−636.

20. Nakamura, J., and Tajima, G. (1995) *J. Biol. Chem. 270*, 17350−17354.
21. Rauch, B., von Chak, D., and Hasselbach, W. (1978) *FEBS Lett. 93*, 65−68.
22. Sumida, M., Wang, T., Mandel, F., Froehlich, J. P., and Schwartz, A. (1978) *J. Biol. Chem. 253*, 8772−8777.
23. Inesi, G. (1987) *J. Biol. Chem. 262*, 16338−16342.
24. Petithory, J. R., and Jencks, W. P. (1988a) *Biochemistry 27*, 5553−5564.
25. Orlowski, S., and Champeil, P. (1991) *Biochemistry 30*, 352−361.
26. Moutin, M. J., and Dupont, Y. (1991) *J. Biol. Chem. 266*, 5580−5586.
27. Lee, A. G., Baker, K., Khan, Y. M., and East, J. M. (1995) *Biochem. J. 305*, 225−231.
28. Bayley, P., Ahlström, P., Martin, S. R., and Forsen, S. (1984) *Biochem. Biophys. Res. Commun. 120*, 185−191.
29. Tsien, R. T. (1980) *Biochemistry 19*, 2396−2404.
30. Champeil, P. (1997) *Biophys. J. 72*, A124.
31. Champeil, P., Riollet, S., Orlowski, S., Guillain, F., Seebregts, C. J., and McIntosh, D. B. (1988) *J. Biol. Chem. 263*, 12288−12294.
32. Martin, S. R., Andersson Teleman, A., Bayley, P. M., Drakenberg, T., and Forsen, S. (1985) *Eur. J. Biochem. 151*, 543−550.
33. Rosenfeld, S. S., and Taylor, E. W. (1985) *J. Biol. Chem. 260*, 242−251.
34. Suko, J., Wyskovsky, W., Pidlich, J., Hauptner, R., Plank, B., and Hellmann, G. (1986) *Eur. J. Biochem. 159*, 425−434.
35. Kilhoffer, M. C., Kubina, M., Travers, F., and Haiech, J. (1992) *Biochemistry 31*, 8098−8106.
36. Martin, S. R., Maune, J. F., Beckingham, K., and Bayley, P. M. (1992) *Eur. J. Biochem. 205*, 1107−1114.
37. Forge, V., Mintz, E., and Guillain, F. (1993a) *J. Biol. Chem. 268*, 10953−10960.
38. Quast, U., Labhardt, A. M., and Doyle, V. M. (1984) *Biochem. Biophys. Res. Commun. 123*, 604−611.
39. Champeil, P., Combettes, L., Berthon, B., Doucet, E., Orlowski, S., and Claret, M. (1989) *J. Biol. Chem. 264*, 17665−17673.
40. Naraghi, M., and Neher, E. (1997) *Biophys. J. 72*, A367.
41. Caldwell, P. C. (1970) in *Calcium and Cellular Function* (Cuthbert, A. W., Ed.) pp 10−12, MacMillan, New York.
42. Tsien, R. T., and Pozzan, T. (1989) *Methods Enzymol. 172*, 230−262.
43. Martell, A. E., and Smith, R. M. (1974) *Critical Stability Constants*, Vols. 1 and 3, Plenum Press, NY.
44. Wolff, H. U. (1983) *Experientia 29*, 241−249.
45. Stefan, L., and Hasselbach, W. (1987) *Z. Naturforsch. 42c*, 641−652.
46. Combettes, L., Claret, M., and Champeil, P. (1993) *Cell Calcium, 14*, 279−292.
47. Champeil, P., and Guillain, F. (1986) *Biochemistry 25*, 7623−7633.
48. Fujimori, T., and Jencks, W. P. (1992) *J. Biol. Chem. 267*, 18475−18487.
49. Orlowski, S., and Champeil, P. (1993) *FEBS Lett. 328*, 296−300.
50. Forbush, B. (1988) *Prog. Clin. Biol. Res. 268A*, 229−248.
51. Pick, U., and Karlish, S. J. (1982) *J. Biol. Chem. 257*, 6120−6126.
52. McIntosh, D. B., Ross, D. C., Champeil, P., and Guillain, F. (1991) *Proc. Natl. Acad. Sci. U.S.A. 88*, 6437−6441.
53. Henderson, I. M. J., Khan, Y. M., East, J. M., and Lee, A. G. (1994a) *Biochem. J. 297*, 615−624.
54. Masuda, H., and de Meis, L. (1973) *Biochemistry 12*, 4581−4585.
55. Guillain, F., Champeil, P., and Boyer, P. D. (1984) *Biochemistry 23*, 4754−4761.
56. Stahl, N., and Jencks, W. P. (1987) *Biochemistry 26*, 7654−7667.
57. Champeil, P. (1993) *Biophys. J. 64*, A353.
58. Tanford, C., Reynolds, J. A., and Johnson, E. A. (1985) *Proc. Natl. Acad. Sci. U.S.A 82*, 4688−4692.
59. Brandl, C. J., Green, N. M., Korczak, B., and Mac Lennan, D. H. (1986) *Cell 44*, 597−607.
60. de Foresta, B., Champeil, P., and le Maire, M. (1990) *Eur. J. Biochem. 194*, 383−388.
61. Gryczynski, I., Wiczk, W., Inesi, G., Squier, T., and Lakowicz, J. R. (1989) *Biochemistry 28*, 3490−3498.
62. Michelangeli, F., Orlowski, S., Champeil, P., Grimes, E. A., East, J. M., and Lee, A. G. (1990) *Biochemistry 29*, 8307−8312.
63. Starling, A. P., East, J. M., and Lee, A. G. (1993) *Biochemistry 32*, 1593−1600.
64. de Foresta, B., Henao, F., and Champeil, P. (1992) *Eur. J. Biochem. 209*, 1023−1034.
65. de Foresta, B., Henao, F., and Champeil, P. (1994) *Eur. J. Biochem. 223*, 359−369.

BI9709699